PNAS RESEARCH ARTICLE | CHEMISTRY MICROBIOLOGY

Molecular responses during bacterial filamentation reveal inhibition methods of drug-resistant bacteria

Dongxue Zhang[a], Fan Yin[a], Qin Qin[b], and Liang Qiao[a,1]

Edited by Dianne Newman, California Institute of Technology, Pasadena, CA; received January 20, 2023; accepted May 22, 2023

Bacterial antimicrobial resistance (AMR) is among the most significant challenges to current human society. Exposing bacteria to antibiotics can activate their self-saving responses, e.g., filamentation, leading to the development of bacterial AMR. Understanding the molecular changes during the self-saving responses can reveal new inhibition methods of drug-resistant bacteria. Herein, we used an online microfluidics mass spectrometry system for real-time characterization of metabolic changes of bacteria during filamentation under the stimulus of antibiotics. Significant pathways, e.g., nucleotide metabolism and coenzyme A biosynthesis, correlated to the filamentation of extended-spectrum beta-lactamase-producing *Escherichia coli* (ESBL-*E. coli*) were identified. A cyclic dinucleotide, c-di-GMP, which is derived from nucleotide metabolism and reported closely related to bacterial resistance and tolerance, was observed significantly up-regulated during the bacterial filamentation. By using a chemical inhibitor, ebselen, to inhibit diguanylate cyclases which catalyzes the synthesis of c-di-GMP, the minimum inhibitory concentration of ceftriaxone against ESBL-*E. coli* was significantly decreased. This inhibitory effect was also verified with other ESBL-*E. coli* strains and other beta-lactam antibiotics, i.e., ampicillin. A mutant strain of ESBL-*E. coli* by knocking out the *dgcM* gene was used to demonstrate that the inhibition of the antibiotic resistance to beta-lactams by ebselen was mediated through the inhibition of the diguanylate cyclase DgcM and the modulation of c-di-GMP levels. Our study uncovers the molecular changes during bacterial filamentation and proposes a method to inhibit antibiotic-resistant bacteria by combining traditional antibiotics and chemical inhibitors against the enzymes involved in bacterial self-saving responses.

antimicrobial resistance | microfluidics | mass spectrometry | metabolomics | proteomics

Significance

Bacterial filamentation is one of the most important bacterial SOS responses to antibiotic drugs and contributes to the development of antimicrobial resistance. Understanding the mechanism of the bacterial SOS responses is crucial to control the development of antibiotic-resistant bacteria. We uncovered key molecular changes during bacterial filamentation induced by antibiotics using real-time metabolomics by online microfluidics mass spectrometry and proteomic analysis of bacterial cells in microfluidic chips. Based on the multiomics analysis, we identified key pathways related to the bacterial filamentation and further developed a method to inhibit antibiotic-resistant bacteria by combining traditional antibiotics and chemical inhibitors against the enzymes involved in the bacterial self-saving responses.

The discovery of antibiotics was enormous success of medicine in the 20th century (1). However, misuse of antibiotics gradually results in the emergence of bacterial antimicrobial resistance (AMR), which is considered a serious global problem threatening public health and leading to financial loss (2). Extended-spectrum beta-lactamase (ESBL)-producing bacteria are one type of the most dangerous antibiotic-resistant bacteria with the ability to hydrolyze third-generation cephalosporins (3). According to the 2,019 Antibiotic Resistance Threats Report from the Centers for Disease Control and Prevention (CDC) in the United States, ESBL-producing Enterobacteriaceae were estimated to trigger 197,400 cases and 9,100 deaths annually in the United States and were classified into the category of "serious threats" (4). In addition, there is no new class of antibiotic drugs against gram-negative bacteria approved over the past 50 y (5). Consequently, developing novel bacterial inhibition methods is of great importance.

Exposing bacteria to antibiotics can accelerate the emergence of AMR and spread of antibiotic-resistant bacteria (6). Under the antibiotic stimulus, bacterial SOS responses can be activated for self-saving (7). Filamentation is one of the bacterial SOS responses against the antibiotic stimulus (8) and is a survival strategy of bacteria in the circumstance of antibiotics (9). Yao et al. reported that *Escherichia coli* can experience four processes when killed by beta-lactam antibiotics, i.e., filamentation, bulge formation, bulge arrest, and cell lysis (10). Bos et al. further found that at subinhibitory concentrations of ciprofloxacin, *E. coli* can change their shape to filaments and propagate daughter cells with stronger AMR (11). Based on single-cell experiments and theoretical modeling, Banerjee et al. demonstrated that morphological changes of bacterial cells can reduce the bacterial uptake of antibiotics, which is a feedback strategy of bacteria to adapt to antibiotics (12). Therefore, bacteria can better overcome the stress of antibiotics and recover to a state of growth with the morphological changes.

Microfluidics has been developed rapidly since the 1990s (13). Various manipulations, such as bacterial culture, treatment, and separation, can be integrated into a small chip which can be coupled with various analytical techniques (14). By designing adequate

Author affiliations: [a]Department of Chemistry, Shanghai Stomatological Hospital, and Institutes of Biomedical Sciences, Fudan University, Shanghai 200000, China; and [b]Changhai Hospital, The Naval Military Medical University, Shanghai 200433, China

Author contributions: L.Q. designed research; D.Z. and F.Y. performed research; Q.Q. contributed new reagents/analytic tools; D.Z. analyzed data; and D.Z. and L.Q. wrote the paper.

The authors declare no competing interest.

This article is a PNAS Direct Submission.

[1]To whom correspondence may be addressed. Email: liang_qiao@fudan.edu.cn.

This article contains supporting information online at https://www.pnas.org/lookup/suppl/doi:10.1073/pnas.2301170120/-/DCSupplemental.

Published June 26, 2023.

microchips, rapid analysis of bacterial morphological dynamic responses to antibiotics has been achieved (15–20). However, observing morphology alone is insufficient. It is necessary to disclose the diverse mechanisms of antibiotics-induced bacterial SOS responses at the molecular level. In our previous work, we designed a gradient microfluidic chip and integrated it with matrix-assisted laser desorption/ionization time-of-flight mass spectrometry to study the protein expression differences between bacteria in different morphologies during antibiotic treatment and identified a panel of protein biomarkers of the corresponding morphological changes (21). In comparison with proteins, metabolites are more dynamic and can reflect the real-time holistic state of biological systems. Changes in bacterial metabolic status can influence their susceptibility to antibiotics and can provide intuitive information about AMR generation (22–24).

Herein, we used an online microfluidics mass spectrometry system to characterize in real time the metabolic changes of ESBL-*E. coli* during filamentation in the presence of ceftriaxone sodium (CEF). The cultured bacteria with or without morphological changes were in situ lysed in the microfluidic chip. Bacterial intracellular metabolites were then online analyzed by electrospray ionization mass spectrometry (ESI-MS). Specific metabolic changes, e.g., in the nucleotide metabolism and coenzyme A (CoA) biosynthesis, during the bacterial filamentation were revealed. We further characterized the proteomic changes of the ESBL-*E. coli* during the filamentation, and the results also suggested the significance of these pathways. A cyclic dinucleotide, c-di-GMP (bis(3′,5′)-cyclic dimeric guanosine monophosphate), which is derived from the nucleotide metabolism and reported closely related to bacterial resistance and tolerance, was observed significantly up-regulated during the bacterial filamentation. By using a chemical inhibitor, ebselen, to inhibit diguanylate cyclases which catalyzes the synthesis of c-di-GMP, the minimum inhibitory concentrations (MICs) of CEF and ampicillin sodium (AMP) against the ESBL-*E. coli* were significantly decreased, which suggested an inhibition method of antibiotic-resistant bacteria by combining traditional antibiotic drugs and chemical inhibitors against the enzymes involved in the antibiotics-induced bacterial SOS responses. The mechanism of the inhibition of the antibiotic resistance to beta-lactams by ebselen was further studied by using a mutant strain of ESBL-*E. coli* without the *dgcM* gene.

Results

Online Microfluidics Mass Spectrometry Characterization of Bacterial Metabolites during Morphological Changes. An asymmetry-sandwich-filtration microfluidic device, composed of a polymethyl methacrylate (PMMA) holder, two polydimethylsiloxane (PDMS) layers with serpentine channels, and a piece of polyethylene terephthalate (PET) membrane with 220 nm pores between the two PDMS layers, was designed and fabricated for bacterial culture under the stimulus of antibiotics (Fig. 1*A* and *SI Appendix*, Fig. S1). Bacterial cells were loaded in the microfluidic device and stayed in the upper channel of the device. Then, culture medium containing antibiotics was infused through the microfluidic device, and filamentation of the bacterial cells was observed from the observation zone (Fig. 1 *A* and *B*). To analyze the metabolites in the bacterial cells, a lysis buffer was injected into the microfluidic chip to extract the bacterial metabolites for online ESI-MS analysis via an electrospray microchip (Fig. 1*C* and *SI Appendix*, Fig. S2).

ESBL-*E. coli* clinically isolated strain (CH 20160920) by Changhai Hospital (*SI Appendix*, Figs. S3 and S4 and Table S1) was used to demonstrate this method. ESBL-*E. coli* (initial concentration ~5×10^8 CFU mL^{-1}, 50 μL) was cultured in the microfluidic device by injecting fresh tryptic soy broth (TSB) medium with or without CEF (2 mg mL^{-1}) continuously (0.5 μL min^{-1}) for 4 h. Six biological replicates were performed on each group. Under these two culture conditions, filamentous elongated bacterial cells (threadlike group) and shape-unchanged bacterial cells (rod-like group) were observed from the observation zone of the microfluidic chip (Fig. 2*A* and *SI Appendix*, Fig. S5). Approximately 89.6% ± 1.8% (n = 6) ESBL-*E. coli* cells were in the threadlike shape in the presence of CEF in the microfluidic chip, and no bacterial cells turned into the threadlike shape in the absence of CEF (*SI Appendix*, Fig. S6). Metabolites in the bacteria were online detected using ESI-MS. Features within 200–2000 *m/z* from the rod-like and threadlike bacterial cells were recorded (Fig. 2*B* and *SI Appendix*, Fig. S7), wherein distinctive features could be observed on the zoomed mass spectra, e.g., *m/z* = 301.1, 308.2, 312.1, 425.3, 689.0, 718.0, and 744.6, with total peak intensity (*m/z* 200 to 2,000) normalized to 100% (Fig. 2*C*). A total of 391 features were detected by the online microfluidics mass spectrometry from the rod-like and threadlike groups. By principal component analysis (PCA) (Fig. 2*D*) and partial least squares–discriminant analysis (PLS-DA) (Fig. 2*E*), the mass spectral features from the rod-like and threadlike bacterial cells could be well clustered into two discriminative groups, indicating that the integrated metabolic state of ESBL-*E. coli* was significantly perturbed during the filamentation. Sixty-five significant features were detected between the rod-like and threadlike bacterial cells with variable importance in projection scores >0.8. From the significant features, 26 differential metabolites were identified based on the accurate mass measurement using a high-resolution TripleTOF mass spectrometer and tandem MS using a linear ion trap (*SI Appendix*, Table S2). The differential metabolites were then subjected to pathway analysis using the BioCyc database (https://biocyc.org/). It was found that metabolic changes were focused on nucleotide metabolism, pantothenate and CoA biosynthesis, arginine degradation, glutathione synthesis, etc. (Fig. 2*F*).

Proteomic Changes during the Filamentation of ESBL-*E. coli*. In order to comprehensively explore the metabolic changes of the bacteria during filamentation, protein variations were also studied. For proteomic analysis, ESBL-*E. coli* cells were cultured with or without CEF in the microfluidic chip in the same way as the metabolomic analysis to form threadlike and rod-like bacterial cells. Then, the bacterial cells in different morphologies were flushed out of the microfluidic chip and collected separately. The intracellular proteins of the two groups of bacterial cells were extracted and characterized by proteomic analysis. Normalization was performed with the total ion chromatogram (TIC). Three biological replicates were performed on each group. A total of 2,693 proteins were identified and quantified from the rod-like and threadlike groups (Dataset S1). Proteins from the rod-like and threadlike cells were clustered into two discriminative groups by score plots of PCA (Fig. 3*A*), indicating that the proteomic state of ESBL-*E. coli* was also significantly perturbed during the filamentation. According to the volcano plot, there were 1,212 proteins with significant regulation [fold change (FC) > 1.5 or < 0.66 and *P*-value < 0.05 by the *t* test adjusted with the Benjamini–Hochberg method] between the threadlike and the rod-like groups (Fig. 3*B* and Dataset S2). According to the functional analysis of the significant proteins using the Clusters of Orthologous Groups of proteins (COG) database, the significant proteins prominently participate in energy production and conversion, amino acid transport and metabolism, and transcription (Fig. 3*C*). The three function classes were proved with fluctuations in the proteomic

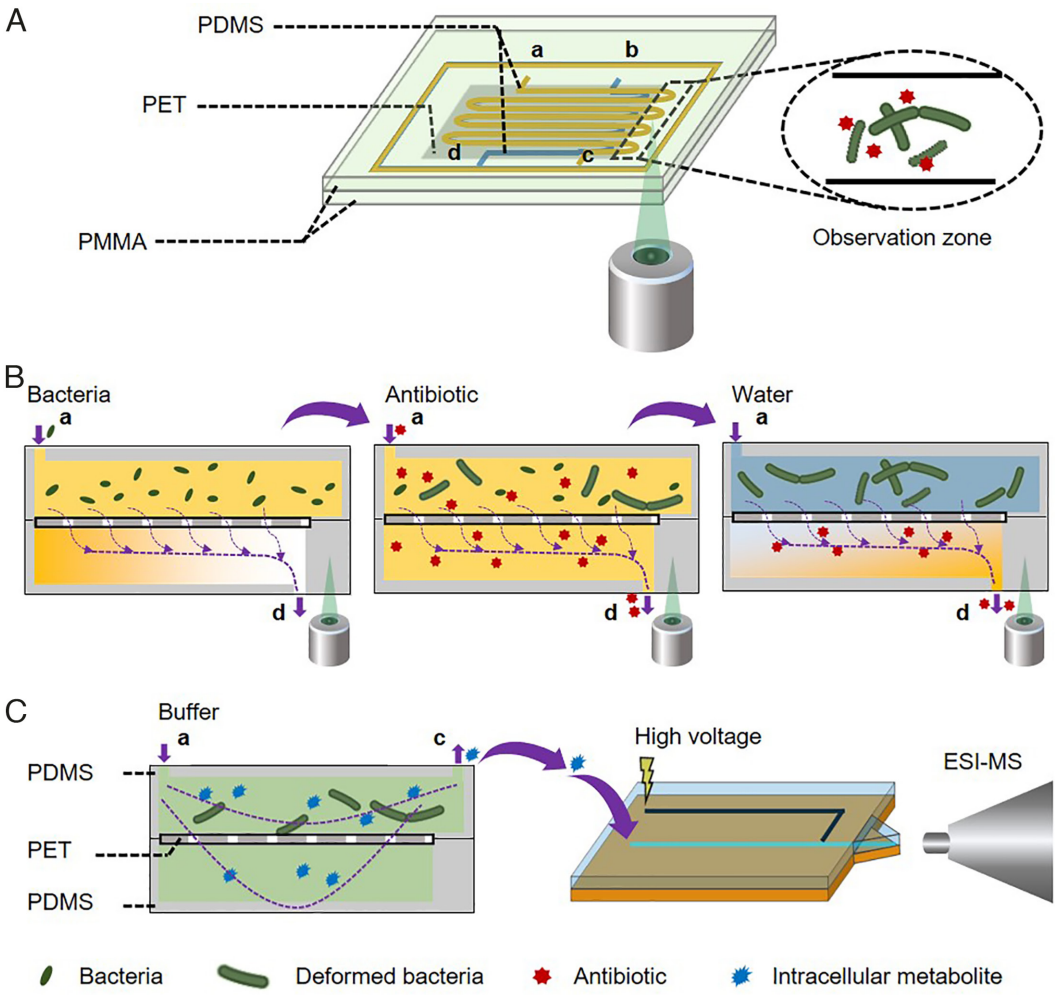

Fig. 1. Schematic illustration of the online microfluidics mass spectrometry for real-time characterization of metabolites during bacterial morphological changes. (*A*) Asymmetry-sandwich-filtration microfluidic device for bacterial culture under the stimulus of antibiotics. (*B*) Bacteria loading, infusion of culture medium containing antibiotics, and washing of culture medium. (*C*) Extraction of bacterial metabolites for online ESI-MS analysis.

study of colistin-tolerant *Pseudomonas aeruginosa* biofilms (25). Resistance to beta-lactams has been reported to comprise a series of responses, including protein translation, posttranslational modifications, energy metabolism, and repair mechanisms (26). All the biological responses were found with significantly regulated proteins during the morphological changes of the ESBL-*E. coli*. Besides, 85 differential proteins were involved in the biogenesis of the cell wall, membrane, and envelope, in consistence with the phenomenon of the morphological elongation. It should be noted that both the proteomic and the metabolomic results suggested the significance of CoA biosynthesis and nucleotide metabolism during the filamentation of ESBL-*E. coli.*

Pathway Analysis Incorporating Metabolomic and Proteomic Data. Incorporating the pathway enrichment results of metabolites and proteins, differential metabolites and proteins were both identified in CoA biosynthesis, nucleotide metabolism, and amino acid metabolism. We summarized the metabolic and proteomic changes in CoA biosynthesis and nucleotide metabolism in Fig. 4 and *SI Appendix*, Figs. S8 and S9. Focusing on the biosynthesis of pantothenate and CoA, metabolites, including glutathione (GSH), 4′-phospho-pantetheine and dephospho-CoA, were up-regulated in the threadlike ESBL-*E. coli*, while (R)-4′-phospho-pantothenoyl-L-cysteine was down-regulated. Enzymes involved in the pathway, including cytosol aminopeptidase (PepA), peptidase B (PepB), and coenzyme A biosynthesis bifunctional protein CoaBC (dfp), were up-regulated, while pantothenate kinase (CoaA), acyl carrier protein phosphodiesterase (AcpH), and 4′-phosphopantetheinyl transferase AcpT (AcpT) were down-regulated. In the GSH metabolism, GSH is converted into L-cysteinyl-glycine and further forms L-cysteine under the catalysis of PepA and PepB. In the CoA biosynthesis, under the action of dfp, L-cysteine and (R)-4′-phospho-pantothenate, which is derived from (R)-pantothenate catalyzed by CoaA, turn into (R)-4′-phospho-pantothenoyl-L-cysteine and 4′-phospho-pantetheine in sequence. 4′-Phospho-pantetheine is then converted into dephospho-CoA, which is the upstream metabolite of CoA. Although we did not detect CoA directly, the upregulation of 4′-phospho-pantetheine and dephospho-CoA and the down-regulation of AcpT and AcpH suggested an accumulation of CoA during the filamentation of the bacteria. CoA is a metabolic integrator and a thiol with low molecular weight to protect bacteria from reactive oxygen species (ROS) (27) generated in the presence of antibiotics (28, 29). It was reported that multidrug resistance could be induced in *E. coli* by stimulating the bacterial cells with the ROS generated by subinhibitory concentration of antibiotics (30).

In nucleotide metabolism, metabolites, such as cytidine, uridine, and guanosine, as well as enzymes such as Protein UshA (UshA) and cytidine deaminase (cdd) were down-regulated, while many

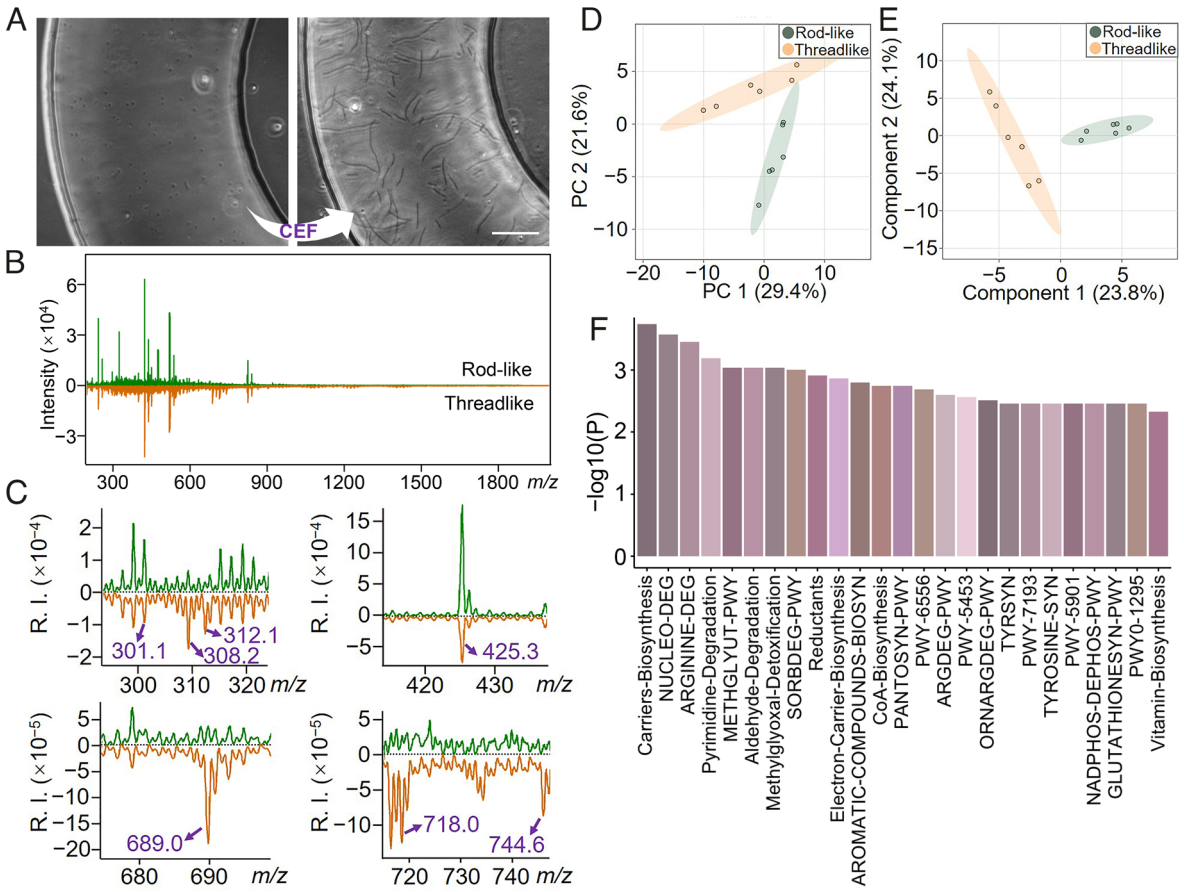

Fig. 2. Online microfluidics mass spectrometry characterization of bacterial metabolites. (*A*) Rod-like and threadlike ESBL-*E. coli* in microchannels (Scale bar: 50 μm). (*B*) Mass spectra of metabolites from the rod-like and threadlike ESBL-*E. coli* averaged from six biological replicates. (*C*) Zoomed normalized mass spectra of ESBL-*E. coli* in rod-like (green) and threadlike (orange) averaged from six biological replicates (R.I.: relative intensity). Normalization was performed with total peak intensity (*m/z* 200 to 2,000) to 100%. Plots of (*D*) PCA and (*E*) PLS-DA of the mass spectral features from the rod-like and threadlike bacterial cells (six biological replicates per group). (*F*) Pathway enrichment of the differential metabolites between the rod-like and threadlike cells using the BioCyc database (https://biocyc.org/).

enzymes, e.g., amidophosphoribosyltransferase (PurF), adenylosuccinate lyase (PurB), adenylate cyclase (CyaA), diguanylate cyclase DgcM (DgcM), diguanylate cyclase DgcJ (DgcJ), cyclic di-GMP phosphodiesterase PdeF (PdeF), cyclic di-GMP phosphodiesterase PdeR (PdeR), and cyclic di-GMP phosphodiesterase PdeK (PdeK), were up-regulated significantly in the threadlike ESBL-*E. coli*. In the nucleotide metabolism, 5-phosphoribosyl 1-pyrophosphate (PRPP) is turned into inosine 5′-monophosphate (IMP) via a series of reactions catalyzed by a number of enzymes including PurF and PurB. The IMP can be consumed in different ways. In one way, adenosine 5′-triphosphate (ATP) can be generated from IMP and then further converted to 3′,5′-cyclic AMP (adenosine 3′,5′-cyclic monophosphate, cAMP) under the catalysis of CyaA. In the other ways, IMP can be converted into guanosine 5′-monophosphate (GMP) and then to guanosine 5′-triphosphate (GTP). The GTP can be further converted to 3′,5′-cyclic GMP (guanosine 3′,5′-cyclic monophosphate, cGMP) and c-di-GMP under the catalysis of CyaA, and diguanylate cyclases (DGCs) such as DgcM and DgcJ, respectively. Under the catalysis of c-di-GMP phosphodiesterases (PDEs), such as PdeF, PdeR and PdeK, c-di-GMP can be hydrolyzed into 5′-phosphoguanylyl-(3′,5′)-guanosine (5′-pGpG). In *E. coli*, high concentrations of 5′-pGpG have been reported to inhibit the enzyme PdeF (31). C-di-GMP, cGMP, and cAMP all belong to the nucleotide second messengers, which regulate several key processes required for bacterial adaptation (32). Among them, c-di-GMP is a ubiquitous second messenger used by many bacteria that controls cell cycle progression, motility, surface adaptation, biofilm production, virulence, and antibiotic tolerance (33–36), so the molecule is closely related to bacterial resistance and tolerance and deserves attention in bacterial AMR research. We did not detect c-di-GMP by untargeted metabolomics based on the online microfluidics mass spectrometry. In order to characterize the abundance regulation of c-di-GMP during bacterial filamentation, we used mass spectrometry-based targeted analysis that has higher sensitivity to detect the abundance variation of c-di-GMP under the stimulus of antibiotics. The relative abundance of c-di-GMP in the threadlike ESBL-*E. coli* with the stimulus of CEF was significantly more abundant than that in rod-like bacteria (Fig. 4*D* and *SI Appendix*, Fig. S10).

Amino acid metabolism was also significantly perturbed during the morphological changes. The up- or downregulation of key enzymes and metabolites in the pathways of amino acid metabolism is summarized in *SI Appendix*, Figs. S8 and S9. Serine acetyltransferase (CysE) is a component of bacterial cysteine synthase complex, involved in the cysteine and methionine metabolism, and has been proposed as a potential target of antibiotic drugs (37). In the threadlike bacteria, CysE was down-regulated significantly, which was beneficial to biofilm formation (38). Inducible ornithine decarboxylase (SpeF), an enzyme involved in the putrescine and spermidine biosynthesis pathways, was highly expressed by the threadlike bacteria compared to the rod-like ones. This enzyme catalyzes the synthesis of putrescine from its precursor arginine,

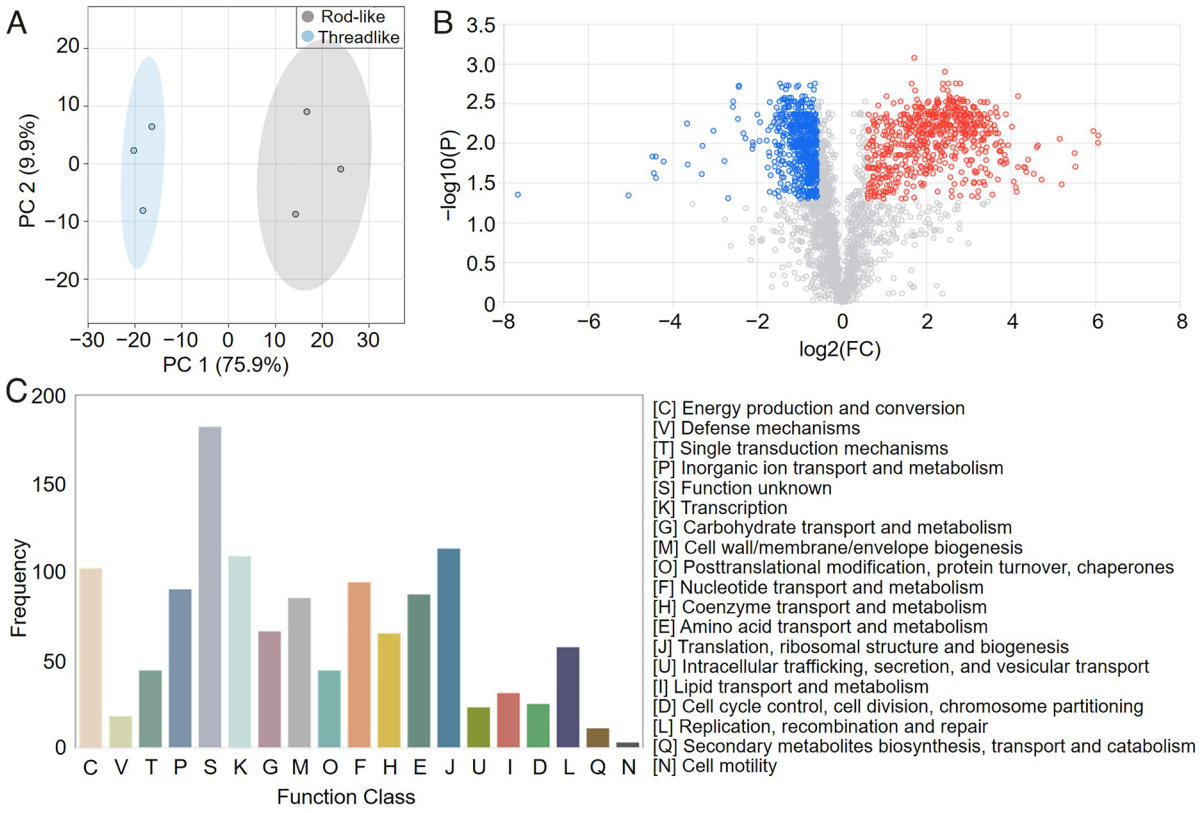

Fig. 3. Proteomic analysis of ESBL-*E. coli* in rod-like and threadlike morphologies. (*A*) Plots of PCA of the rod-like and threadlike samples based on proteome data (three biological replicates). (*B*) Volcano plots of identified proteins between the rod-like and threadlike groups, with significant upregulation (FC > 1.5 and *P*-value < 0.05) in red and significant downregulation (FC < 0.66 and *P*-value < 0.05) in blue. Gray: not significant. The *P* value was calculated by the *t* test adjusted with the Benjamini–Hochberg method. (*C*) COG functional annotation of the 1,212 proteins with significant variations between the threadlike and the rod-like groups. Frequency: the number of proteins belonging to a Function Class.

while putrescine and arginine are involved in the biofilm formation and c-di-GMP synthesis (39, 40).

Inhibition of Bacterial Antibiotic Resistance by Inhibiting the Synthetase of c-di-GMP. From the multiomics-based pathway analysis, the nucleotide metabolism was found significantly perturbed during the filamentation of ESBL-*E. coli*. The molecule c-di-GMP is derived from nucleotide metabolism and plays an important role in the bacterial tolerance to antibiotics (33). The level of c-di-GMP is controlled by two classes of enzymes, DGCs and PDEs, for the synthesis and degradation of c-di-GMP, respectively (41). Although PDEs were also up-regulated like DGCs during the bacterial filamentation, PDEs such as PdeF can be inhibited by its catalytic product of c-di-GMP, 5′-pGpG (42), indicating that their activity is mutually balanced. In our study, c-di-GMP was accumulated during bacterial filamentation and exhibited upregulation. To investigate the role of c-di-GMP in the bacterial tolerance to antibiotics, we implemented a strategy to reduce the level of c-di-GMP by inhibiting the synthetase of c-di-GMP, DGCs. Ebselen is a chemical inhibitor of DGCs by covalently modifying cysteine residues (43, 44). It is a synthetic organoselenium drug molecule, clinically used as an anti-inflammatory agent, and has recently been reported exhibiting promising inhibitory effect against COVID-19 in cell-based assays (45). It has been used to kill gram-positive bacteria with the principle of obstructing antioxidant ability of bacteria by inhibiting thioredoxin reductase (TrxR) (46) and to destroy fungi by means of reducing GSH concentration in microbe to dysregulate redox homeostasis (47). Nevertheless, it cannot inhibit gram-negative bacteria (48).

We demonstrated that ebselen at 50 μM does not significantly influence the growth of the ESBL-*E. coli* (Fig. 5 *A* and *B*) and used this concentration for further research. We disclosed that ebselen can indeed decrease the MIC of CEF against the ESBL-*E. coli*. In the presence of ebselen, the MIC of CEF against the ESBL-*E. coli* declined by at least four times (Fig. 5*C*). This bacterial inhibition effect was also demonstrated with another ESBL-*E. coli* strain (49) (CICC 10663, China Center of Industrial Culture Collection, Beijing, China, Fig. 5*D*), as well as with another type of beta-lactam antibiotics, AMP (Fig. 5 *E* and *F*). Consequently, ebselen has a great potential in improving the efficiency of beta-lactam antibiotics to inhibit ESBL-producing bacteria.

We further investigated the mechanism of the inhibitory effect of ebselen on bacteria under the treatment of antibiotics. When treated with ebselen, the abundance of c-di-GMP in ESBL-*E. coli* cells stimulated with CEF was down-regulated (Fig. 5*G*), demonstrating that ebeslen can inhibit the DGCs and hence decrease the generation of c-di-GMP. Among the DGCs detected in this work, DgcM was significantly up-regulated during the bacterial filamentation. DgcM was reported to assist in the synthesis of c-di-GMP and participate in biofilm regulation (50). To study the role of DgcM in the bacterial tolerance to antibiotics, a mutant strain of ESBL-*E. coli* (CH 20160920) was constructed that knocked out the *dgcM* gene, namely ESBL/Δ*dgcM*. As shown in Fig. 5*H*, in the presence of ebselen (50 μM), the growth of the ESBL/Δ*dgcM* strain was not significantly interfered. Different from the significant effect of ebselen on the MIC of CEF against the strain CH 20160920 (Fig. 5*C*), the MICs of CEF against the mutant strain ESBL/Δ*dgcM* with or without ebselen were very close (Fig. 5*I*).

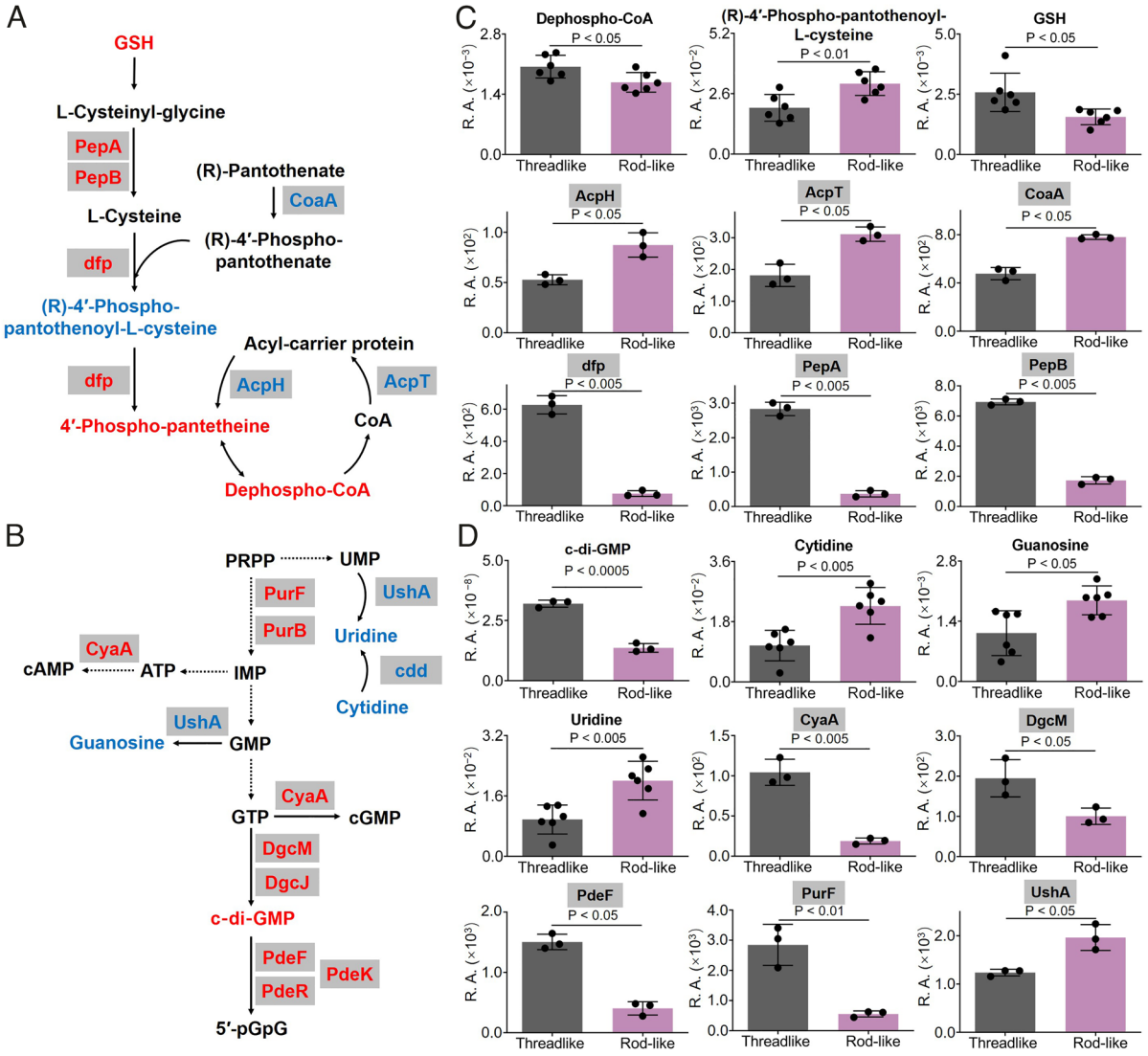

Fig. 4. Illustration of the perturbed pathways during the filamentation of ESBL-*E. coli*. Pathways of (*A*) CoA biosynthesis and (*B*) nucleotide metabolism (gray filling: protein; none filling: metabolite; red: upregulation; blue: downregulation; black: undetected). The relative abundance of part of the metabolites and proteins involved in (*C*) the CoA biosynthesis pathway and (*D*) the nucleotide metabolism pathway between the rod-like and threadlike bacteria. Error bars represent SD (six biological replicates for metabolites and three biological replicates for proteins, gray filling: protein; none filling: metabolite). R.A.: relative abundance. The *P* value was calculated by the *t* test adjusted with the Benjamini–Hochberg method. The relative abundance of c-di-GMP was calculated based on the most intensive fragment peak of c-di-GMP in MS/MS spectra normalized by the summed intensity of the corresponding full MS scan, explained in detail in *SI Appendix*, Fig. S10. Relative abundances of other metabolites and proteins involved in the pathways are shown in *SI Appendix*, Figs. S8 and S9.

All these results demonstrated the significance of c-di-GMP and DgcM in the bacterial tolerance to antibiotics and suggested that the inhibitory effect of ebselen on the bacterial resistance to beta-lactams was mainly through the inhibition of DgcM and hence the production of c-di-GMP.

Discussion

Escalating AMR makes common medicines ineffective and has been a severe problem for a long time. The number of infections caused by antibiotic-resistant bacteria annually in the United States climbed from 2 million in 2013 to 2.8 million in 2019 (4, 51). ESBL-producing Enterobacteriaceae are classified in the category of "serious threats" by the CDC in the United States and may be classified in the most dangerous category in the future if there is not proper public health surveillance and prevention (4). Carbapenem is one of the few remaining antibiotics that can kill ESBL-producing bacteria. However, extensive usage of carbapenem can induce the emergence of common "superbugs," i.e., carbapenem-resistance bacteria (52), which are resistant to most existing antibiotic drugs. Therefore, developing novel bacterial inhibition methods is of great importance.

SOS response is closely related to the generation of persister cells, population-wide tolerance, and shielding (53). It can support bacterial persistence in two ways, i.e., adjusting persister cell formation by complementary stress signaling and resuscitating persister cells by supplying diverse DNA repair functions (54). Persistence and tolerance are similar phenomena in bacteria where bacteria can survive in the presence of bactericidal antibiotic concentrations, and the two terms are often interchangeable in studies that focus only on molecular mechanisms (55). Quorum sensing and biofilm formation are also affiliated with SOS response (56). Bacteria in biofilm lifestyle have stronger tolerance to antibiotics, and the evolution of bacterial AMR in biofilm lifestyle is faster than in planktonic lifestyle (57). In contrast to tolerance which describes bacteria surviving under a transient exposure to antibiotics, resistance is the ability of bacteria to replicate in the presence of antibiotics (58). Bacterial tolerance can promote the emergence of resistance (59,

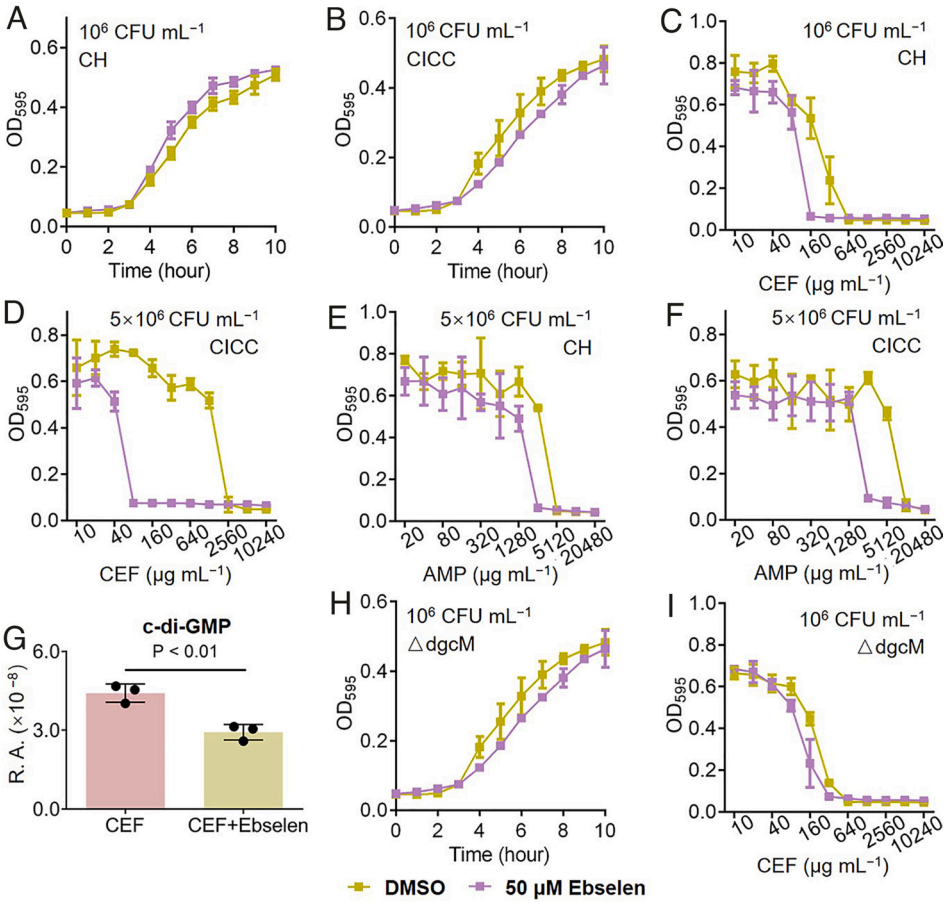

Fig. 5. Inhibitory effect of ebselen on drug-resistant bacteria. The growth curve of ESBL-*E. coli* strain (*A*) CH 20160920 and (*B*) CICC 10663 with or without 50 μM ebselen. The MIC of CEF against ESBL-*E. coli* strain (*C*) CH 20160920 and (*D*) CICC 10663 with or without 50 μM ebselen. The MIC of AMP against ESBL-*E. coli* strain (*E*) CH 20160920 and (*F*) CICC 10663 with or without 50 μM ebselen. (*G*) The relative abundance of c-di-GMP in ESBL-*E. coli* (CH 20160920) under CEF (2 mg mL^{-1}) stimulation with or without the treatment of 50 μM ebselen. The *P* value was calculated by the *t* test adjusted with the Benjamini–Hochberg method. (*H*) The growth curve of CH 20160920 mutant strain ESBL/*ΔdgcM* and (*I*) the MIC of CEF against ESBL/*ΔdgcM* with or without 50 μM ebselen. OD595: optical density at 595 nm. CH: CH 20160920; CICC: CICC 10663; DMSO: the culture condition without ebselen; 50 μM ebselen: the culture condition with 50 μM ebselen. Error bars represent the SD (three biological replicates). R.A.: relative abundance. Initial concentrations of ESBL-*E. coli* are shown in the figures. The relative abundance of c-di-GMP was calculated based on the most intensive fragment peak of c-di-GMP in MS/MS spectra normalized by the summed intensity of the corresponding full MS scan, explained in detail in *SI Appendix*, Fig. S10.

60). For example, antibiotic tolerance has been reported to facilitate the development of antibiotic resistance in *E. coli* by increasing survival and mutation rates in the presence of antibiotics (61). In this work, on the basis of the phenomenon of SOS-associated filamentation, we used microfluidics mass spectrometry to conduct research on bacterial tolerance, and based on the findings from multiomics analysis, we developed a method to inhibit the drug-resistant bacteria.

Changes on metabolites and proteins of bacteria induced by antibiotics can provide meaningful information on bacterial SOS response mechanism study. Compared to transcriptome and genome, metabolome and proteome can better represent the function and phenotype of bacteria. Functional proteins, such as those composing the peptidoglycan-based bacterial cell wall, participating in energy metabolism, taking part in the response to oxidative stress, and involving in amino acid biosynthesis, were found with significant changes when bacteria were stimulated by antibiotics (62, 63). In comparison with genes and proteins, metabolites are more dynamic and can reflect the real-time holistic state of biological systems. Changes in bacterial metabolic states can influence the susceptibility of bacteria to antibiotics and can provide intuitive information of AMR generation (22). Previous studies on metabolic responses of *Staphylococcus aureus* in the presence of antibiotics have revealed extensive effects of the antibiotic stimulus in metabolism pathways, like D-alanine metabolism (23), center carbon and amino acid metabolism, and synthesis of peptidoglycan, purine, and pyrimidine (24). By integrating metabolic and proteomic approaches, new drug targets for the inhibition of bacteria may be disclosed, and new antibiotics may be developed.

Quenching methods are crucial in microbial metabolomic studies due to the dynamic changes of metabolites. The most commonly used quenching methods for microbial metabolomics include fixation by perchloric acid and cold methanol and separation by filtration and centrifugation (64). The fixation by acids or organic solvents can induce leakage of intracellular metabolites, resulting in inaccurate identification and quantification of metabolites. Centrifugation and filtration-based methods are time consuming, wherein changes of active metabolites may occur (65). In this work, we cultured bacteria in the presence of antibiotics in a microfluidic chip. Bacterial morphology and growth under the circumstance of antibiotics in the microfluidic chip can be continuously monitored. The cultured bacteria were in situ lysed in the microfluidic chip, avoiding tedious procedures, such as centrifugation, in bulk culture-based experiments. The most essential advantage of this chip is that it can be coupled with ESI-MS to realize online metabolites analysis. Intracellular metabolites in real-time state were detected by mass spectrometry, which reduced the variation of metabolites,

achieved precise determination, and minimized possible exogenous influence to metabolomics analysis.

Mass spectrometry can provide fruitful molecular information closely related to microbial physiology. Nevertheless, the numbers of bacterial cells cultured in microfluidic devices are usually small, making the MS-based proteome and metabolome analyses difficult. In this work, bacterial intracellular metabolites were analyzed by direct infusion ESI-MS without separation techniques. This strategy is robust, but the coverage of metabolites is limited compared to comprehensive metabolomics analysis by liquid chromatography tandem mass spectrometry (LC-MS/MS). In future development, microfluidic chips filled with microparticles or nanoparticles can be developed for metabolite separation (66), connected to bacterial culture chips, and integrated with ESI-MS to form an online system for metabolite extraction, separation, and detection, enabling deep coverage of metabolites. For proteomic analysis, advances in sample processing, nanoflow separation, as well as ultrasensitive mass spectrometers with gas-phase separation (such as timsTOF) pave the way for single-cell proteome analysis (67). For example, the nanoPOTS platform, a sample preparation system based on microdroplet, can reduce the sample loss and improve protein recovery and the efficiency of sample processing (68, 69). Besides, enzymatic reactors in microfluidic chips can be used for online protein denaturation and digestion prior to LC-MS/MS analysis (70). In this work, we used microfluidics mass spectrometry to study bacterial tolerance to antibiotics. The microfluidics mass spectrometry technique can also be used for bacterial classification, AMR detection, studies of bacterial physiological responses to other stresses (such as drugs, immune cells, and symbiotic microorganisms), drug screening, bacteria-bacteria/host cell interaction studies, bacteria-related disease mechanism studies, and the exploration of new therapeutic approaches.

In summary, we characterized the molecular changes of ESBL-*E. coli* during filamentation induced by antibiotics using an online microfluidics mass spectrometry system and demonstrated the significant roles of c-di-GMP and DGCs in bacterial tolerance to antibiotics. We have also proposed a therapeutic method combining ebselen with beta-lactam antibiotics like CEF to kill ESBL-*E. coli*, wherein ebselen can inhibit DGCs to decrease the generation of c-di-GMP and hence the bacterial resistance to antibiotics. We would expect that a similar strategy can be applied to the study of other antibiotic-resistant bacteria and that such an approach of combining traditional antibiotics with chemical inhibitors against enzymes involved in bacterial SOS responses can open an avenue for clinical treatment of bacterial infection.

Materials and Methods

Details of the materials and methods used in this work are described in *SI Appendix, SI Text, Materials and Methods*.

Design and Fabrication of Microfluidic Chips. The sandwich microfluidic device for bacterial culture consisted of two pieces of PMMA slices, two layers of PDMS, and a PET membrane (*SI Appendix*, Fig. S1). The PDMS layers were designed by AutoCAD and fabricated following the standard soft lithography and molding technology. The polyimide microchip for ESI was designed using AutoCAD (*SI Appendix*, Fig. S2) and manufactured by laser engraving.

Online Microfluidics Mass Spectrometry Analysis of Metabolites from ESBL-*E. coli* with/without CEF Stimulation. Fifty microliter ESBL-*E. coli* (~5 × 10^8 CFU mL^{-1}) was injected into the sandwich microfluidic device. TSB medium with or without CEF (2 mg mL^{-1}) was injected (0.5 μL min^{-1}) into the microfluidic chip to culture and stimulate the bacterial cells for 4 h continuously. Sterile water and metabolite extraction buffer (75% acetonitrile, 23% deionized water, and 2% acetic acid) were used to remove culture medium and extract bacterial intracellular metabolites, respectively. Metabolites of bacterial cells were directed to the polyimide microchip for ESI-MS analysis.

Proteomic Analysis of ESBL-*E. coli* Cultured in the Microfluidic Chip with/without CEF Stimulation. For proteomic analysis, bacterial cells were cultured in the sandwich microfluidic chip under the same condition as the metabolomic analysis. Phosphate buffered saline (PBS) was used to wash the bacterial cells out of the microfluidic chip. Proteins of bacteria were extracted, reduced, alkylated, and tryptic digested in sequence. Peptides were desalted, quantified, and analyzed using a nano-high-performance liquid chromatography tandem mass spectrometry (HPLC-MS/MS) system under the parallel accumulation-serial fragmentation combined with data-independent acquisition (diaPASEF) mode.

C-di-GMP Detection. Bacterial cells (~5 × 10^8 CFU mL^{-1}, 50 μL) were loaded into the sandwich microfluidic chip and cultured with pure TSB, with TSB and CEF (2 mg mL^{-1}), with TSB, CEF (2 mg mL^{-1}), and dimethyl sulfoxide (DMSO, 0.5%), or with TSB, CEF (2 mg mL^{-1}), ebselen (50 μM), and DMSO (0.5%) for 4 h, respectively. PBS was used to wash the bacterial cells out of the microfluidic chip. Metabolites were extracted by three freeze–thaw cycles, and c-di-GMP was detected by targeted ESI-MS analysis.

Data Analysis. Direct infusion MS data for online metabolite detection were processed with an R package MALDIquant. Statistical analyses were performed using MetaboAnalyst. Pathway enrichment analyses were performed using BioCyc. Metabolite identification was performed using Metabolite identification and Dysregulated Network Analysis (MetDNA) and Human Metabolome Database (HMDB). Proteomics data were processed and analyzed by Spectronaut. Function annotation was carried out using Gene Ontology annotation.

Preparation of the Mutant Strain ESBL/Δ*dgcM*. The *dgcM* knockout strain of ESBL-*E. coli* (CH 20160920) was produced by homologous recombination.

Bacterial Growth Curve and MIC Detection in the Presence of Ebselen. For growth curve determination, 10 μL bacterial cells were cultured in 100 μL TSB medium with 0.5% DMSO or with 50 μM ebselen and 0.5% DMSO at 37 °C for 10 h. MIC was detected using the micro-broth dilution method. Ten microliter bacterial cells were added into 100 μL TSB medium with 0.5% DMSO and antibiotics in gradient concentrations or 100 μL TSB medium with 50 μM ebselen, 0.5% DMSO, and antibiotics in gradient concentrations and cultured at 37 °C for 20 h. All the experiments were performed in 96-well microtiter plates. OD595 was measured by the Microplate Reader to detect the growth curve and MIC value.

Data, Materials, and Software Availability. All the proteome data have been deposited to ProteomeXchange via the iProX (71, 72) partner repository with the dataset identifiers IPX0005704001/PXD039235 (https://proteomecentral.proteomexchange.org/cgi/GetDataset?ID=PXD039235) (73).

ACKNOWLEDGMENTS. This work is supported by the National Natural Science Foundation of China (22022401, 22074022, and 21934001). We would like to acknowledge Yan-Jun Liu and Ya-Jun Wang from Fudan University in bright-field imaging of bacterial cells. We would also like to acknowledge Chengpin Shen and Xiaoqing Wang from Shanghai Omicsolution Co., Ltd., for their support in proteomic analysis.

1. O. O. Komolafe, Antibiotic resistance in bacteria - an emerging public health problem. *Malawi Med. J.* **15**, 63–67 (2003).
2. A. T. B. Abadi, A. A. Rizvanov, T. Haertle, N. L. Blatt, World health organization report: Current crisis of antibiotic resistance. *Bionanoscience* **9**, 778–788 (2019).
3. D. L. Paterson, R. A. Bonomo, Extended-spectrum beta-lactamases: A clinical update. *Clin. Microbiol. Rev.* **18**, 657–686 (2005).
4. CDC, Antibiotic resistance threats in the United States (CDC Centers for Disease Control and Prevention, Department of Health and Human Services, 2019).
5. P. A. Smith *et al.*, Optimized arylomycins are a new class of Gram-negative antibiotics. *Nature* **561**, 189–194 (2018).
6. D. I. Andersson, D. Hughes, Microbiological effects of sublethal levels of antibiotics. *Nat. Rev. Microbiol.* **12**, 465–478 (2014).
7. C. Miller *et al.*, SOS response induction by beta-lactams and bacterial defense against antibiotic lethality. *Science* **305**, 1629–1631 (2004).
8. R. P. Jaktaji, S. Pasand, Overexpression of SOS genes in ciprofloxacin resistant Escherichia coli mutants. *Gene* **576**, 115–118 (2016).

9. S. S. Justice, D. A. Hunstad, L. Cegelski, S. J. Hultgren, Morphological plasticity as a bacterial survival strategy. *Nat. Rev. Microbiol.* **6**, 162–168 (2008).
10. Z. Yao, D. Kahne, R. Kishony, Distinct single-cell morphological dynamics under beta-lactam antibiotics. *Mol. Cell* **48**, 705–712 (2012).
11. J. Bos *et al.*, Emergence of antibiotic resistance from multinucleated bacterial filaments. *Proc. Natl. Acad. Sci. U.S.A.* **112**, 178–183 (2015).
12. S. Banerjee *et al.*, Mechanical feedback promotes bacterial adaptation to antibiotics. *Nat. Phys.* **17**, 403–409 (2021).
13. G. M. Whitesides, The origins and the future of microfluidics. *Nature* **442**, 368–373 (2006).
14. D. Zhang, H. Bi, B. Liu, L. Qiao, Detection of pathogenic microorganisms by microfluidics based analytical methods. *Anal. Chem.* **90**, 5512–5520 (2018).
15. J. Choi *et al.*, A rapid antimicrobial susceptibility test based on single-cell morphological analysis. *Sci. Transl. Med.* **6**, 267ra174 (2014).
16. T. Kong *et al.*, Adhesive tape microfluidics with an autofocusing module that incorporates CRISPR interference: Applications to long-term bacterial antibiotic studies. *ACS Sens.* **4**, 2638–2645 (2019).
17. B. Li *et al.*, Gradient microfluidics enables rapid bacterial growth inhibition testing. *Anal. Chem.* **86**, 3131–3137 (2014).
18. P. Sabhachandani *et al.*, Integrated microfluidic platform for rapid antimicrobial susceptibility testing and bacterial growth analysis using bead-based biosensor via fluorescence imaging. *Microchim. Acta* **184**, 4619–4628 (2017).
19. Z. Pilat *et al.*, Microfluidic cultivation and laser tweezers raman spectroscopy of E-coli under antibiotic stress. *Sensors* **18**, 1623 (2018).
20. X. Jiang *et al.*, Studies of the drug resistance response of sensitive and drug-resistant strains in a microfluidic system. *Integr. Biol.* **6**, 143–151 (2014).
21. D. Zhang *et al.*, MALDI-TOF characterization of protein expression mutation during morphological changes of bacteria under the impact of antibiotics. *Anal. Chem.* **91**, 2352–2359 (2019).
22. J. M. Stokes, A. J. Lopatkin, M. A. Lobritz, J. J. Collins, Bacterial metabolism and antibiotic efficacy. *Cell Metab.* **30**, 251–259 (2019).
23. K. Schelli, F. Y. Zhong, J. J. Zhu, Comparative metabolomics revealing Staphylococcus aureus metabolic response to different antibiotics. *Microb. Biotechnol.* **10**, 1764–1774 (2017).
24. K. Doerries, R. Schlueter, M. Lalk, Impact of antibiotics with various target sites on the metabolome of Staphylococcus aureus. *Antimicrob. Agents Chemother.* **58**, 7151–7163 (2014).
25. S. L. Chua *et al.*, Selective labelling and eradication of antibiotic-tolerant bacterial populations in Pseudomonas aeruginosa biofilms. *Nat. Commun.* **7**, 10750 (2016).
26. B. Peng, H. Li, X. Peng, Proteomics approach to understand bacterial antibiotic resistance strategies. *Expert Rev. Proteomic.* **16**, 829–839 (2019).
27. I. Gout, Coenzyme A: A protective thiol in bacterial antioxidant defence. *Biochem. Soc. Trans.* **47**, 469–476 (2019).
28. M. A. Lobritz *et al.*, Antibiotic efficacy is linked to bacterial cellular respiration. *P. Natl. Acad. Sci. U.S.A.* **112**, 8173–8180 (2015).
29. A. Gutierrez *et al.*, beta-lactam antibiotics promote bacterial mutagenesis via an RpoS-mediated reduction in replication fidelity. *Nat. Commun.* **4**, 1610 (2013).
30. M. A. Kohanski, M. A. DePristo, J. J. Collins, Sublethal antibiotic treatment leads to multidrug resistance via radical-induced mutagenesis. *Mol. Cell* **37**, 311–320 (2010).
31. M. M. Lacey, J. D. Partridge, J. Green, Escherichia coli K-12 YfgF is an anaerobic cyclic di-GMP phosphodiesterase with roles in cell surface remodelling and the oxidative stress response. *Microbiology* **156**, 2873–2886 (2010).
32. D. Kalia *et al.*, Nucleotide, c-di-GMP, c-di-AMP, cGMP, cAMP, (p)ppGpp signaling in bacteria and implications in pathogenesis. *Chem. Soc. Rev.* **42**, 305–341 (2013).
33. U. Romling, C. Balsalobre, Biofilm infections, their resilience to therapy and innovative treatment strategies. *J. Intern. Med.* **272**, 541–561 (2012).
34. U. Jenal, A. Reinders, C. Lori, Cyclic di-GMP: Second messenger extraordinaire. *Nat. Rev. Microbiol.* **15**, 271–284 (2017).
35. H. Almblad *et al.*, Bacterial cyclic diguanylate signaling networks sense temperature. *Nat. Commun.* **12**, 1986 (2021).
36. C. Opoku-Temeng, H. O. Sintim, Targeting c-di-GMP signaling, biofilm formation, and bacterial motility with small molecules. *Methods Mol. Biol.* **1657**, 419–430 (2017).
37. B. Rosa *et al.*, Combination of SAXS and protein painting discloses the three-dimensional organization of the bacterial cysteine synthase complex, a potential target for enhancers of antibiotic action. *Int. J. Mol. Sci.* **20**, 5219 (2019).
38. G. Sturgill, C. M. Toutain, J. Komperda, G. A. O'Toole, P. N. Rather, Role of CysE in production of an extracellular signaling molecule in Providencia stuartii and Escherichia coli: Loss of cysE enhances biofilm formation in Escherichia coli. *J. Bacteriol.* **186**, 7610–7617 (2004).
39. P. R. Guerra *et al.*, Putrescine biosynthesis and export genes are essential for normal growth of avian pathogenic Escherichia coli. *BMC Microbiol.* **18**, 226 (2018).
40. Z. Liu, S. S. Hossain, Z. Morales Moreira, C. H. Haney, Putrescine and its metabolic precursor arginine promote biofilm and c-di-GMP synthesis in pseudomonas aeruginosa. *J. Bacteriol.* **204**, e0029721 (2022).
41. R. Hengge, Principles of c-di-GMP signalling in bacteria. *Nat. Rev. Microbiol.* **7**, 263–273 (2009).
42. K. Heo *et al.*, A pGpG-specific phosphodiesterase regulates cyclic di-GMP signaling in Vibrio cholerae. *J. Biol. Chem.* **298**, 101626 (2022).
43. O. J. Lieberman, M. W. Orr, Y. Wang, V. T. Lee, High-throughput screening using the differential radial capillary action of ligand assay identifies ebselen as an inhibitor of diguanylate cyclases. *ACS Chem. Biol.* **9**, 183–192 (2014).
44. C. Opoku-Temeng, J. Zhou, Y. Zheng, J. Su, H. O. Sintim, Cyclic dinucleotide (c-di-GMP, c-di-AMP, and cGAMP) signalings have come of age to be inhibited by small molecules. *Chem. Commun.* **52**, 9327–9342 (2016).
45. Z. Jin *et al.*, Structure of M(pro) from SARS-CoV-2 and discovery of its inhibitors. *Nature* **582**, 289–293 (2020).
46. X. Ren, L. Zou, J. Lu, A. Holmgren, Selenocysteine in mammalian thioredoxin reductase and application of ebselen as a therapeutic. *Free Radic. Biol. Med.* **127**, 238–247 (2018).
47. S. Thangamani *et al.*, Ebselen exerts antifungal activity by regulating glutathione (GSH) and reactive oxygen species (ROS) production in fungal cells. *Biochim. Biophys. Acta Gen. Subj.* **1861**, 3002–3010 (2017).
48. S. Thangamani, W. Younis, M. N. Seleem, Repurposing clinical molecule ebselen to combat drug resistant pathogens. *PLoS One* **10**, e0133877 (2015).
49. D. Zhang *et al.*, Microfluidic filter device coupled mass spectrometry for rapid bacterial antimicrobial resistance analysis. *Analyst* **146**, 515–520 (2021).
50. M. Hoekzema, C. Romilly, E. Holmqvist, E. G. H. Wagner, Hfq-dependent mRNA unfolding promotes sRNA-based inhibition of translation. *EMBO J.* **38**, e101199 (2019).
51. CDC, Antibiotic resistance threats in the United States (CDC Centers for Disease Control and Prevention, Department of Health and Human Services, 2013).
52. M. E. Rupp, P. D. Fey, Extended spectrum β-lactamase (ESBL)-producing enterobacteriaceae. *Drugs* **63**, 353–365 (2003).
53. Z. Podlesek, D. Žgur Bertok, The DNA damage inducible SOS response is a key player in the generation of bacterial persister cells and population wide tolerance. *Front. Microbiol.* **11**, 1785 (2020).
54. A. Harms, E. Maisonneuve, K. Gerdes, Mechanisms of bacterial persistence during stress and antibiotic exposure. *Science* **354**, aaf4268 (2016).
55. N. Q. Balaban *et al.*, Definitions and guidelines for research on antibiotic persistence. *Nat. Rev. Microbiol.* **17**, 441–448 (2019).
56. Z. Baharoglu, D. Mazel, SOS, the formidable strategy of bacteria against aggressions. *FEMS Microbiol. Rev.* **38**, 1126–1145 (2014).
57. O. Ciofu, C. Moser, P. Jensen, N. Høiby, Tolerance and resistance of microbial biofilms. *Nat. Rev. Microbiol.* **20**, 621–635 (2022).
58. A. Brauner, O. Fridman, O. Gefen, N. Q. Balaban, Distinguishing between resistance, tolerance and persistence to antibiotic treatment. *Nat. Rev. Microbiol.* **14**, 320–330 (2016).
59. I. Levin-Reisman *et al.*, Antibiotic tolerance facilitates the evolution of resistance. *Science* **355**, 826–830 (2017).
60. J. Liu, O. Gefen, I. Ronin, M. Bar-Meir, N. Q. Balaban, Effect of tolerance on the evolution of antibiotic resistance under drug combinations. *Science* **367**, 200–204 (2020).
61. E. M. Windels *et al.*, Bacterial persistence promotes the evolution of antibiotic resistance by increasing survival and mutation rates. *ISME J.* **13**, 1239–1251 (2019).
62. D. Jones-Dias *et al.*, Quantitative proteome analysis of an antibiotic resistant Escherichia coli exposed to tetracycline reveals multiple affected metabolic and peptidoglycan processes. *J. Proteomics* **156**, 20–28 (2017).
63. R. Monteiro, M. Hebraud, I. Chafsey, P. Poeta, G. Igrejas, How different is the proteome of the extended spectrum beta-lactamase producing Escherichia coli strains from seagulls of the Berlengas natural reserve of Portugal? *J. Proteomics* **145**, 167–176 (2016).
64. F. R. Pinu, S. G. Villas-Boas, R. Aggio, Analysis of intracellular metabolites from microorganisms: Quenching and extraction protocols. *Metabolites* **7**, 53 (2017).
65. P. Vrabl, D. J. Artmann, C. W. Schinagl, W. Burgstaller, Rapid sample processing for intracellular metabolite studies in Penicillium ochrochloron CBS 123.824: The FiltRes-device combines cold filtration of methanol quenched biomass with resuspension in extraction solution. *Springerplus* **5**, 966 (2016).
66. A. Kecskemeti, A. Gaspar, Particle-based liquid chromatographic separations in microfluidic devices - A review. *Anal. Chim. Acta* **1021**, 1–19 (2018).
67. R. T. Kelly, Single-cell proteomics: Progress and prospects. *Mol. Cell. Proteomics* **19**, 1739–1748 (2020).
68. Y. Zhu *et al.*, Nanodroplet processing platform for deep and quantitative proteome profiling of 10–100 mammalian cells. *Nat. Commun.* **9**, 882 (2018).
69. J. Woo *et al.*, High-throughput and high-efficiency sample preparation for single-cell proteomics using a nested nanowell chip. *Nat. Commun.* **12**, 6246 (2021).
70. J. Sproß, A. Sinz, A capillary monolithic trypsin reactor for efficient protein digestion in online and offline coupling to ESI and MALDI mass spectrometry. *Anal. Chem.* **82**, 1434–1443 (2010).
71. J. Ma *et al.*, iProX: An integrated proteome resource. *Nucleic Acids Res.* **47**, D1211–D1217 (2019).
72. T. Chen *et al.*, iProX in 2021: Connecting proteomics data sharing with big data. *Nucleic Acids Res.* **50**, D1522–D1527 (2022).
73. D. Zhang, L. Qiao, Molecular responses during bacterial filamentation induced by antibiotics. iProX. https://www.iprox.cn/page/project.html?id=IPX0005704000. Deposited 4 January 2023.